JOURNAL OF SOLID STATE CHEMISTRY 44, 1–23 (1982)

Crystal Chemistry of the VA Element Trihalides: Lone Pair, Stereochemistry, and Structural Relationships*

JEAN GALY AND RENÉE ENJALBERT

Laboratoire de Chimie de Coordination du CNRS, 205 route de Narbonne, 31400 Toulouse, France

Received December 20, 1981

The crystal structures of NCl_3, PCl_3, PBr_3, AsF_3, and $AsCl_3$ liquids at room temperature have been recently determined. The data for the last two are reported in the present paper. The structures of the following trihalides are discussed and classified in structural types: AsF_3, SbF_3, αBiF_3, YF_3 (NCl_3, PCl_3, PBr_3, $\beta SbCl_3$, $\beta SbBr_3$, γBiF_3, and $\beta BiCl_3$), $AsBr_3$ ($AsCl_3$, $AsBr_3$, "$\alpha SbCl_3$," and $\alpha SbBr_3$), PI_3 and αAsI_3 (αAsI_3, SbI_3, and BiI_3). Structural relationships have been established between AsF_3 and XeO_3, PX_3E and POX_3 (X = Cl, Br), and $AsBr_3E$ has been compared with $PuBr_3$ and $VOCl_3$. A structural mechanism is proposed for the polymorphic transformation $\alpha SbBr_3 \rightleftarrows \beta SbBr_3$. The $CrCl_3$ structure type is proposed for the high-temperature form of AsI_3 and a mechanism is given for the phase transition $\alpha AsI_3 \rightleftarrows \beta AsI_3$. A proposal is made for a possible high-pressure transformation of the αAsI_3 structure into a VF_3 structure type. The stereochemistry is discussed in terms of coordination polyhedra around M^*; all these trihalides are characterized by a basic molecular unit M^*X_3. The steric effects of the lone pair E carried by M^* is especially emphasized and discussed; two characteristics of E are presented: the centroid of the electronic doublet located by E_c and the sphere of influence located by its center E_s. The correlative variations of M^*–E_c and M^*–E_s are studied according to the nature of M^* (N(III), P(III) to Cl(V), Ga(I) to Br(V), In(I) to Xe(VI), and Tl(I) to Po(IV)).

Introduction

The chemistry and stereochemistry of oxides containing transition elements and elements M^* carrying a lone pair E were an extremely attractive field for one of us (JG) because of the wide variety offered of new compounds apt to be formed and because of the original structures such compounds exhibit. Such an area was investigated through the chemistry based on tellurium(IV) possessing the electronic structure $\{Kr\}4d^{10}5s^2$. The stereochemical influence of the lone pair on tellurium(IV) was readily enhanced and the various crystal structures compared with those "lone pair" elements like Sb(III), Pb(II), etc. (*1*). The various coordination polyhedra of tellurium were investigated by Zemann (*2*) who gave a most valuable contribution to the understanding of tellurium(IV) structural chemistry. A further exhaustive contribution to this field was given by Meunier (*3*).

The lone-pair steric effects have been analyzed in terms of interelectron repulsion by Sidgwick and Powell (*4*). Their theory was modified a few years later by Gillespie and Nyholm (*5*) who assumed lone pairs to be larger than bonding pairs, so that the repulsion between electron pairs decreases as: lone pair–lone pair > lone pair–bonding

* Dedicated to Professor A. F. Wells on his 70th birthday.

0022-4596/82/100001-23$02.00/0

pair > bonding pair–bonding pair (VSEPR theory). The electron pairs are at the corner of a polyhedron with the nucleus at its center, the considerable distortion occurring due to the larger size of the lone pair, sitting in the site normally occupied by a ligand, according to the previous authors. An important and fundamental investigation by *ab initio* calculations was recently performed by Schmiedekamp *et al.* (*6*) on the VSEPR models.

In the area of structural chemistry, a fundamental observation was pointed out by Andersson and Åström (*7*) working in the field of oxides, fluorides, and oxide fluorides of "ns^2 elements": the lone pair in these compounds takes the same volume as an oxide O^{2-} or a fluoride F^- ion. This is easily checked by calculating the volume per anion in "lone pair" compounds. This volume is of the same importance as the one found in transition metal oxides, i.e., 16–18 Å^3, if the lone pairs are taken into account (only true for elements with a single lone pair).

We named the space required by the nonbonded electron pair "*the sphere of influence of the lone pair E,*" which may include the associated cation. Hence the center of this sphere, referred to as E_s, was placed at the vertex of a regular polyhedron, such as a tetrahedron, a trigonal bipyramid, or an octahedron. Then, following these principles, Galy *et al.* (*8*) derived the distance nucleus–E_s for the M^* elements, Ge(II) to Br(V), Sn(II) to Xe(VI), and Tl(I) to Bi(III), after a thorough study of a number of oxide and fluoride structures. The distance nucleus–centroid of the lone pair, i.e., E_c, is consequently somewhat shorter than the distance nucleus–E_s.

In order to extend this analysis of the stereochemical effects of the lone pair E to other ligands fixed on M^* elements, an investigation of the crystal structures of the trihalides of VA elements was attempted. Some of them were not known or poorly defined. A few structures were then determined and refined and are reported in the present paper, together with the results found in the literature.

All these trihalides M^*X_3 are characterized in the gas, liquid, and solid states by a simple pyramidal molecular structure. However, in the solid state, the crystal network exhibits various molecular packings. In Sections I, II, and III of the present study, we will deal with the classification by structural type, with the aim of reporting the general organization of the packing and the structural relationships, and describing the various coordination polyhedra in which the element M^* and its lone pair adopt. The last section will report the characteristics of M^*X_3 molecules and the stereochemical effects of the lone pair E on the structures.

I. M^*F_3 Trifluorides

The first two trifluorides of this series, NF_3 and PF_3, are gaseous at room temperature. The structures of these molecules have only been studied by electron diffraction. AsF_3, SbF_3, and BiF_3 have different structural types, the later showing various polymorphic forms.

AsF_3—A Structural Type

The detailed structure of crystalline AsF_3, liquid at room temperature, was reported by Enjalbert and Galy (*9*) (Table I). The detailed experimental data are developed in Enjalbert's thesis (*10*), some results of which are reported in Appendix I.

AsF_3 crystallizes in the orthorhombic system and the atomic arrangement is shown in Fig. 1 (noncentrosymmetric space group $Pn2_1a$). The AsF_3 unit with its arsenic and three fluorine atoms has approximately the expected C_{3v} symmetry. However, there are six other fluorine neighbors completing a distorted tricapped trigonal prism around AsE.

TABLE I

CRYSTALLOGRAPHIC DATA FOR MOLECULES $M^{*}X_3$

Compound	Molecular weight	Melting point (K)	Liquid specific mass (g cm^{-3})	Crystal specific mass (g cm^{-3})RX	Temperature of X-ray study (K)	Crystal system	Space group	(Unit cell parameters) a (Å)	b (Å)	c (Å)	Volume (Å^3)	Number of molecules/cell	Reliability factor of the structure determination	Reference
NF_3	71.0	66	—	—	—	—	—	—	—	—	—	—	—	
PF_3	88.0	121	—	—	—	—	—	—	—	—	—	—	—	
AsF_3	131.9	267	2.666	3.28	193	Orth.	$Pn2_1a$	7.018(5)	7.315(6)	5.205(6)	267	4	0.055	(*9*)
SbF_3	178.8	565		4.39	293	Orth.	$Ama2$	7.26(1)	7.46(1)	4.95(1)	268	4	0.072	(*13*)
αBiF_3	266.0	1000		8.76	293	Cubic	$P\bar{4}3m$	5.865(6)			202	4	—	(*15*)
γBiF_3	266.0	1000		7.88	293	Orth.	$Pnma$	6.56	7.03	4.86	224	4	—	(*17*)
δBiF_3						Tetra.		7.076		7.350			—	(*16*)
NCl_3	120.4	<233	1.653	2.08	148	Orth.	$Pnma$	7.48(2)	9.35(1)	16.48(2)	1153	12	0.091	(*33*)
PCl_3	137.3	161	1.574	1.99	123	Orth.	$Pnma$	8.0425(8)	9.3691(7)	6.0794(4)	458	4	0.029	(*21*)
$AsCl_3$	181.3	264	2.163	2.62	253	Orth.	$P2_12_12_1$	9.466(3)	11.335(3)	4.289(2)	460	4	0.036	(*19*)
$\beta SbCl_3$	228.1	346		3.14	293	Orth.	$Pnma$	8.111(2)	9.419(1)	6.313(1)	482	4	0.045	(*31*)
$\alpha BiCl_3$	315.3	503		3.89	293	Cubic	$P2_13$	8.14			539	4	—	(*41*)
$\beta BiCl_3$	315.3	503		4.75	293	Orth.	$Pnma$	7.641(2)	9.172(7)	6.291(2)	441	4	0.044	(*32*)
NBr_3	—	—	—	—	—	—	—	—	—	—	—		—	
PBr_3	270.7	233	2.852	3.47	193	Orth.	$Pnma$	8.014(4)	10.026(8)	6.444(4)	518	4	0.034	(*20*)
$AsBr_3$	314.7	306		3.86	293	Orth.	$P2_12_12_1$	10.240(5)	12.200(5)	4.33(1)	541	4	0.19	(*37*)
$\alpha SbBr_3$	361.5	370		4.37	293	Orth.	$P2_12_12_1$	10.12(1)	2.30(1)	4.42(1)	550	4	0.18	(*38*)
$\beta SbBr_3$	361.5	370		4.38	293	Orth.	$Pnma$	8.25(1)	9.96(1)	6.68(1)	549	4	0.104	(*30*)
$\alpha BiBr_3$	448.7	491		3.79	293	Cubic	$P2_13$	9.23			786	4	—	(*41*)
NI_3	394.7	—		—	—	—	—	—	—	—	—		—	
PI_3	411.7	334		4.18	293	Hexag.	$P6_3$	7.133(2)		7.414(2)	327	2	0.065	(*44*)
αAsI_3	455.6	419		4.74	293	Trig.	$R\bar{3}$	7.193(2)		21.372(7)	958	6	0.033	(*46*)
βAsI_3	455.6	419		4.71	393	Trig.	$P3_212$	7.20(5)		21.47(8)	964	6	—	
SbI_3	502.5	443		4.94	293	Trig.	$R\bar{3}$	7.48(2)		20.90(5)	1013	6	0.131	(*49*)
BiI_3	589.5	681		5.81	293	Trig.	$R\bar{3}$	7.514(2)		20.702(7)	1012	6	0.15	

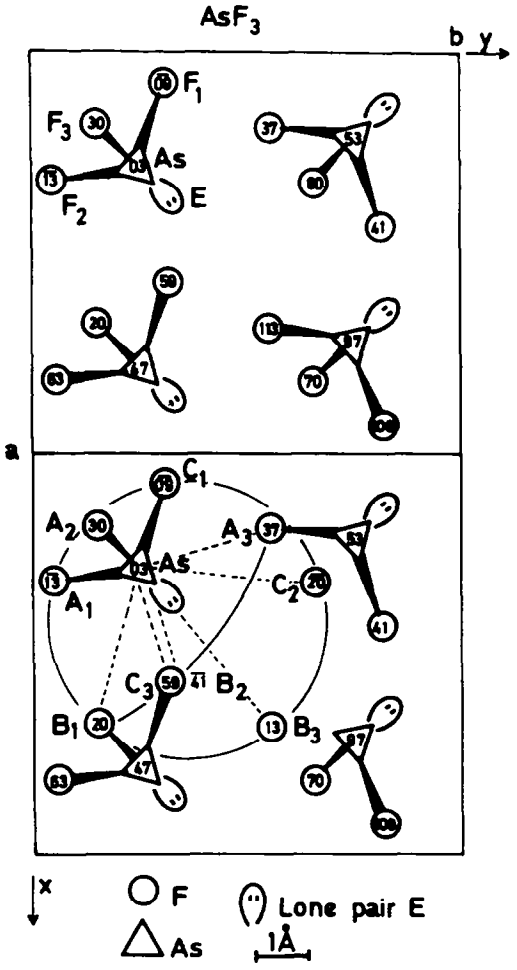

FIG. 1. Projection of the AsF_3 crystal structure onto the (001) plane. Coordination polyhedron around AsE.

If we draw a schematic polyhedron packing of AsF_3 with the trigonal prisms surrounding the lone pair *E*, Fig. 2a is obtained showing layers of alternated prisms along the *a* axis; an important capping summit is indicated to remind us that an arsenic atom of a layer of trigonal prisms is connected to a fluorine of the neighboring unit.

Structural relationship between AsF_3 and XeO_3. XeO_3 is orthorhombic ($a = 6.16, b = 8.11, c = 5.23$ Å, space group $P2_12_12_1$) (*11*). Andersson (*12*) discussed the stereochemistry of valence bonds and the structure of the xenon trioxide together with those of the fluorides XeF_4 and XeF_2.

Xe(VI), like As(III), possesses a lone pair. In Fig. 2b (drawn according to Andersson (*12*)), it is readily seen that, despite some distortion, XeO_3 shows a structural packing remarkably similar to that of AsF_3.

SbF_3—A Structural Type

The crystal structure of SbF_3 was reinvestigated by Edwards (*13*) (Table I). The SbF_3 units are linked through three fluorine bridges to form a three-dimensional net-

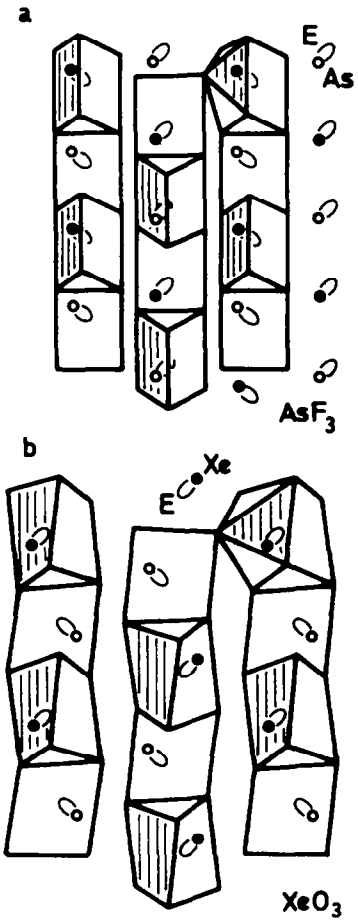

FIG. 2. AsF_3 and XeO_3 crystal structure. Small circles are As(III) or Xe(VI) situated in the capped square pyramid; lone pairs are located in the trigonal prisms.

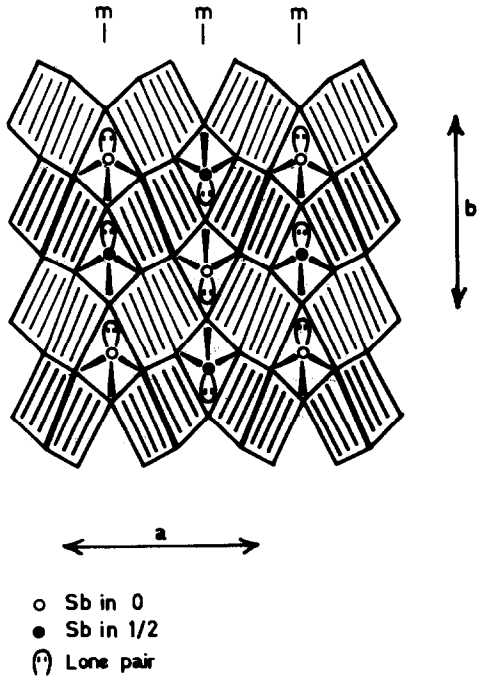

FIG. 3. Packing of fluorine rhombic prisms between the mirror planes in the SbF_3 crystal structure.

work with a distorted trigonal antiprism of fluorine around SbE which reside together with fluorine atoms in mirror planes. The general structure can be described as being composed of layers of fluorine rhombic prisms sharing edges and vertices. The mirrors play the role of "twinning" planes accommodating the Sb atoms. The SbF_3 structure, slightly idealized in this way, is represented in Fig. 3.

BiF_3

Two polymorphs of this ionic fluoride, α and γ, have been structurally characterized.

αBiF_3. αBiF_3 crystallizes in the cubic system (Table I) and gives a polymorphic β form above a transition temperature of 473 K (*14*). According to Hund and Fricke (*15*), in the αBiF_3 structure Bi atoms should be surrounded by eight fluorine atoms forming a cube. In fact, a displacement of bismuth toward one fluoride along the threefold axis of the cube decreases the coordination number to 7 and the fluorine polyhedron around Bi becomes a monocapped trigonal antiprism.

γBiF_3. The orthorhombic γ form (Table I) pertains to an isostructural family including several M^*Cl_3 and M^*Br_3 compounds and classified as a YF_3 structure type described below.

δBiF_3. This phase appears at 5–7 kbars and 20°C when the γ form undergoes shock compression (*16*); it is tetragonal with a = 7.076, c = 7.350 Å (Table I).

II. M^*X_3 Trichlorides and Tribromides

These trihalides can be assigned two main structure types, respectively:

(1) the YF_3 crystal structure:

NCl_3	
PCl_3	PBr_3
$\beta SbCl_3$	$\beta SbBr_3$
γBiF_3	$\beta BiCl_3$

and

(2) the $AsBr_3$ crystal structure:

$AsCl_3$	$AsBr_3$
"$\alpha SbCl_3$"	$\alpha SbBr_3$

The bismuth compounds exhibit a cubic form, the crystal structure of which has not been determined.

YF_3 Structure Type

The YF_3 structure has been determined by Zalkin and Templeton (*17*) (orthorhombic, space group *Pnma*, a = 6.353, b = 6.850, c = 4.393 Å) and can be classified as an anti-Fe_3C type. In the cementite structure, described as an example of chemical twinning in HCP, one C atom is situated in a two-capped trigonal prism of Fe atoms (*18*).

In YF_3 and in their related M^*X_3 the cations, as well as the lone pair, are situated inside the prisms. The idealized picture of this typical structure is given in Fig. 4. In

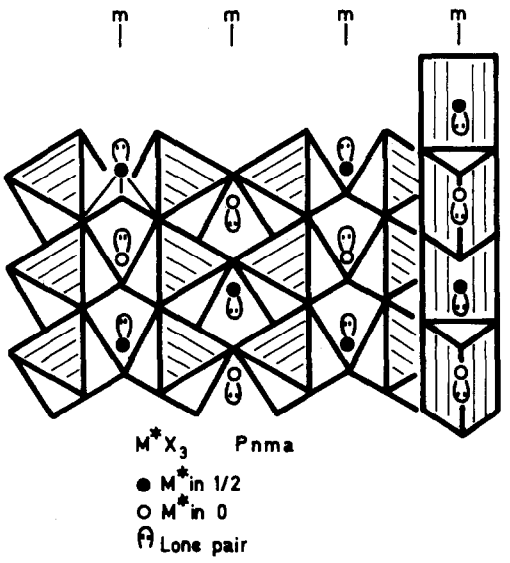

FIG. 4. Idealized projection of a M^*X_3 with YF_3 structure type onto the plane (001). M^* atoms in the mirrors are located in trigonal prisms (right portion of the figure); halogen octahedra are in between the mirror planes.

these M^*X_3 compounds, the molecular entity is maintained and a network results from the peculiar packing of the molecules. The M^* atoms are located in bicapped trigonal prisms of halogens.

PCl_3 and PBr_3. These compounds, liquid at room temperature, have been crystallized *in situ* on an automatic X-ray diffractometer and their structures determined by Enjalbert and Galy (*19, 20*) and Enjalbert *et al.* (*21*) (Table I). An investigation of PCl_3 has also been carried out by Hartl *et al.* (*22*).

A projection onto the plane (100) of this typical orthorhombic structure (space group *Pnma*) is given in Fig. 5. It clearly shows the disposition of the M^*X_3 molecules which possess a mirror plane as a symmetry element. This assertion is supported by nuclear quadrupolar resonance studies on PCl_3 (*23*) and PBr_3 (*24*), since these compounds give only two signals which characterize two crystallographically independent halogens (i.e., two X atoms are related by a symmetry element, namely, the mirror plane of the space group *Pnma*).

Structural relationships with $POCl_3$ and $POBr_3$. These oxyhalides are isostructural with the corresponding trihalides and in the later the lone pair E is substituted for the oxygen atom. $POCl_3$ and $POBr_3$ structures were determined by Olie (*25*) and Olie and Mijlhoff (*26*), respectively, who assigned them a noncentrosymmetric space group. However, a refinement of $POBr_3$ carried out by Templeton and Templeton (*27*), as well as a NQR study by Okuda *et al.* (*28*) confirmed the presence of the mirror plane with *Pnma* as the space group. Such a result may be reasonably extended to $POCl_3$. The X-ray data of these phosphorous oxyhalides are very similar to those of the phosphorous trihalides ones:

$POCl_3$ (*25*): orthorhombic, *Pnma*, a = 9.185(3), b = 9.326(2), c = 5.749(1) Å (corrected space group).

$POBr_3$ (*26*): orthorhombic, *Pnma*, a = 9.467(6), b = 9.938(6), c = 6.192(3) Å.

$\beta SbCl_3$ and $\beta SbBr_3$. The crystal structures of these antimony compounds have been determined by Lindqvist and Niggli (*29*) for $\beta SbCl_3$ and Cushen and Hulme for

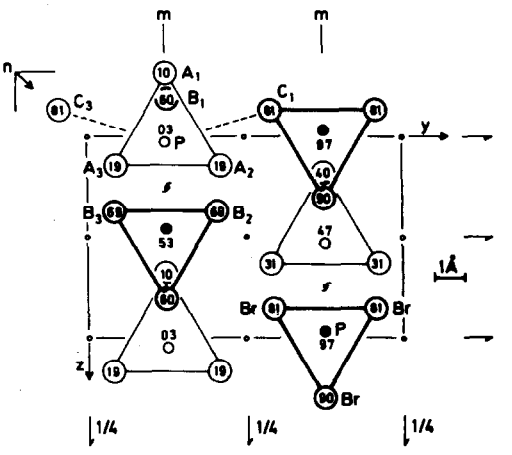

FIG. 5. Ball and spoke projection of the PBr_3 structure onto the plane (100).

$\beta SbBr_3$ (*30*). A refinement of $\beta SbCl_3$ has been recently published by Lipka (*31*). These two halides belong to the YF_3 structure type.

γBiF_3 and $\beta BiCl_3$. γBiF_3 is isostructural with YF_3, as indicated by Zalkin and Templeton (*17*).

From a detailed X-ray single crystal study, Nyburg *et al.* (*32*) claimed $\beta BiCl_3$ belonged to the $Pn2_1a$ space group instead of the most symmetrical *Pnma*. They obtained a very small distortion and, in spite of Hamilton's test, the result supporting $Pn2_1a$ is not very convincing (especially in a crystal structure containing heavy elements such as bismuth) (Table I). But the NQR study (*23*) definitively resolved this problem by showing only two signals, which then implies the *Pnma* space group.

NCl_3—An unexpected superstructure. This compound, investigated by Hartl *et al.* (*33*), crystallizes in the orthorhombic system, space group *Pnma*, with the *c* parameter three times as large as that in the YF_3 structure type (Table I). Consequently, there are three crystallographically independent nitrogen atoms in the cell (N(1), N(2), N(3)) and the NCl_3 molecules still contain the mirror plane as a symmetry element. The packing of these molecules is such that N(1) is located in a large trigonal antiprism and N(2) and N(3) in bicapped trigonal prisms.

A projection on the mirror plane has been prepared to compare this structure with the previous ones. PBr_3 is represented in Fig. 6 and NCl_3 in Fig. 7. These figures clearly show the networks formed by the trigonal prisms in PBr_3 and the trigonal prisms and antiprisms in NCl_3. It is seen that the tripling of the *c* parameter in NCl_3 is due to the tilting of the $N(1)Cl_3$ molecule in the same direction as $N(2)Cl_3$ along the line of chlorine atoms following the direction {100}. The $N(3)Cl_3$ molecules are packed in a way more similar to PBr_3, for example. These figures, especially Fig. 6, directly

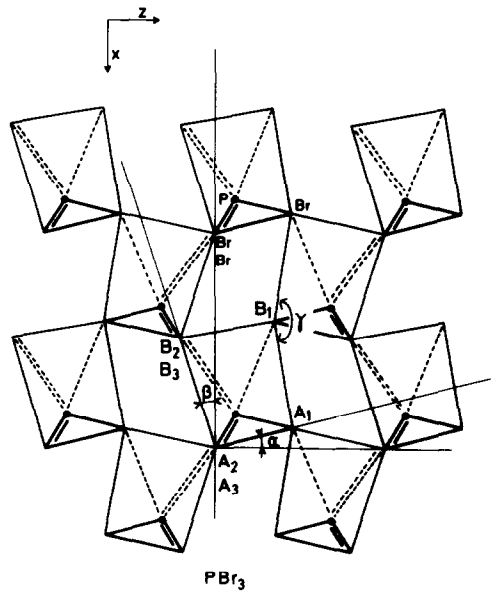

FIG. 6. A layer of M^*X_3 molecules; projection onto the mirror plane (PBr_3 structure) with the M^* atoms in trigonal prisms; α, β, and γ angles indicate the general distortion of the packing.

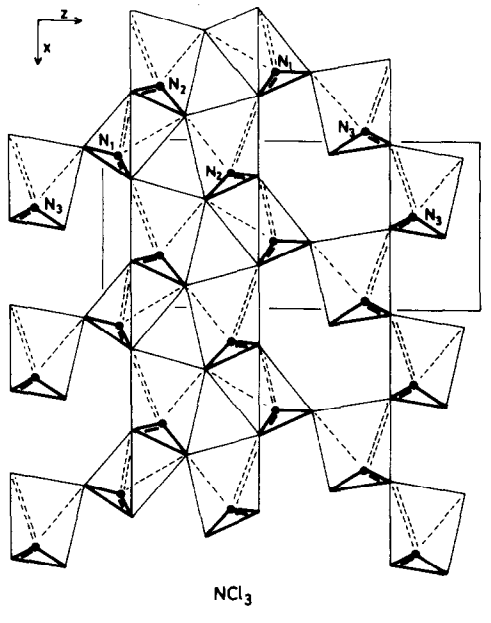

FIG. 7. A layer of NCl_3 molecules; it shows the combination of chlorine trigonal prisms (around N(2) and N(3) atoms) and octahedra (around N(1)) leading to the tripling of the *c* parameter.

concern the whole series of YF_3 structure type compounds and they show how distorted the packing of the trigonal prisms can be.

To evaluate this distortion, we defined the angles α = dihedral angle between the triangle built of the halogens of the M^*X_3 molecule and the plane (100), β = dihedral angle between the rectangular face of the trigonal prism composed of the halogens related by the mirror plane and the plane (001), and γ = the angle between successive halogens belonging to the mirror plane in the {100} direction. These angles are presented in Table II. The corresponding distortion for $POCl_3$ and $POBr_3$ are included for comparison.

$AsBr_3$ Structure Type

This structure was determined in 1935 on a single crystal of arsenic tribromide by Braekken (*34*).

$AsCl_3$ and $AsBr_3$. The crystal structure of $AsCl_3$ has been investigated at low temperature by Enjalbert and Galy (*10,19*) (cf. Appendix II). A drawing of the molecular disposition is given in Fig. 8. The molecules are piled up in the {001} direction as infinite trigonal chains and the arsenic atoms are located in the trigonal prisms. All these

TABLE II

DISTORTION OF THE M^*X_3 PACKING IN YF_3 RELATED STRUCTURES[a]

Compound	$\lvert\alpha\rvert$	$\lvert\beta\rvert$	$\lvert\gamma\rvert$
PCl_3	17	0	150
PBr_3	13	19	160
$\beta SbCl_3$	16	20	152
$\beta SbBr_3$	16	19	151
$\beta BiCl_3$	17	20	144
$N(1)Cl_3$	27	36	153
NCl_3 $N(2)Cl_3$	27	0	154
$N(3)Cl_3$	10	0	153
$POCl_3$	26	13	136
$POBr_3$	26	12	140

[a] α, β, and γ in degrees.

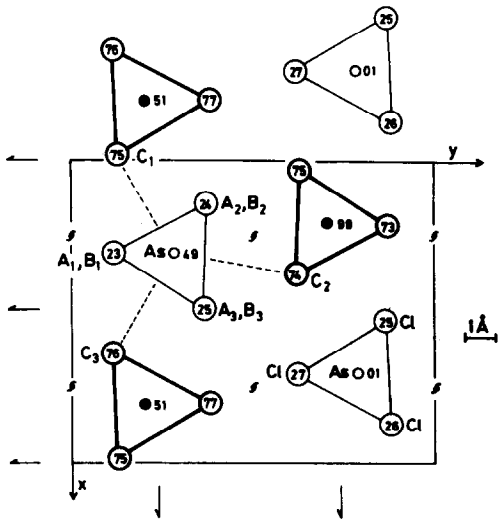

FIG. 8. Detailed projection of the $AsCl_3$ structure onto the plane (001).

chains are parallel, which brings three extra chlorine atoms close to the arsenic and its lone pair. A coordination polyhedron is thus defined as a tricapped trigonal prism.

The $AsBr_3$ structure has been redetermined by Singh and Swaminathan (*35*) and Trotter (*36*) and refined (R = 0.143) by Singh and Swaminathan (*37*).

"$\alpha SbCl_3$" and $\alpha SbBr_3$. The compound "$\alpha SbCl_3$" is reported by Lindqvist and Niggli (*29*) but no X-ray work has been cited.

The structure $\alpha SbBr_3$ has been determined by Cushen and Hulme (*38*).

Structural relationships with $PuBr_3$ and $VOCl_3$. The typical infinite trigonal chains of the M^*X_3 compounds with the $AsBr_3$ structure type are held together by weak interactions and an idealized drawing is given in Fig. 9.

$PuBr_3$ is built up of similar chains (orthorhombic, space group *Ccmm*, a = 12.64, b = 4.10, c = 9.14 Å (*39*)) but, despite similar tricapped trigonal prism coordination polyhedra around the plutonium atoms, the general packing appears different (Fig. 10). Yet, the structure of $VOCl_3$

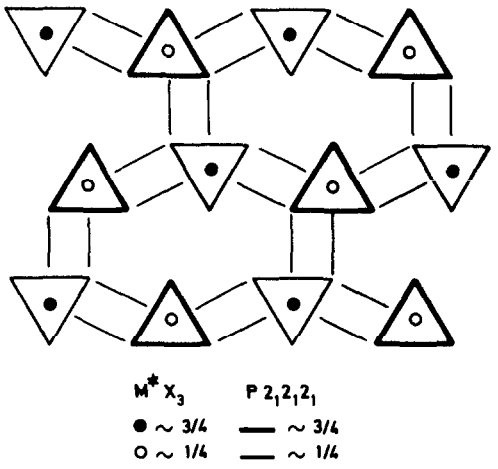

FIG. 9. Ideal packing of the infinite linear chains of M^* filled halogen trigonal prisms with $AsBr_3$ structure type (triangles in projection onto the plane (001)). Thin lines indicate the weak secondary interchain bonding, yielding a tricapped trigonal prism coordination around M^*.

recently investigated in our laboratory by Enjalbert *et al.* (*40*) (orthorhombic, space group *Pnma*, $a = 4.963(1)$, $b = 9.140(4)$, $c = 11.221(5)$ Å at 133 K) seems more closely related to $AsBr_3$. The packing is derived from $AsBr_3$ by a slip affecting every two layers of chains parallel to the plane (100) and by the adjusting of the trigonal chains on the mirror planes (Fig. 11). The VO group is inserted in a bicapped trigonal prism of chlorine atoms.

A possible mechanism for the $\alpha SbBr_3 \rightleftarrows \beta SbBr_3$ *transformation.* The structure of $\alpha SbBr_3$ is represented in Fig. 12a. When each layer B is moved in the direction of the arrow by a vector Br–Br, the arrangement drawn in Fig. 12b is obtained. As indicated in the right portion of the drawing, the infinite trigonal chains containing the antimony atoms and their lone pairs are now separated by empty infinite trigonal chains (indicated with dashed lines in the projection). Half of the antimony atoms may move easily through the rectangular face of trigonal prisms into the opposite empty ones (indicated by arrows). The detail of this operation is further shown in Fig. 13. The parameter along the chains is then doubled and the structure of $\beta SbBr_3$ is obtained (Fig. 14).

The α *form of* $BiCl_3$ *and* $BiBr_3$. According to Wolten and Mayer (*41*), $\alpha BiCl_3$ and

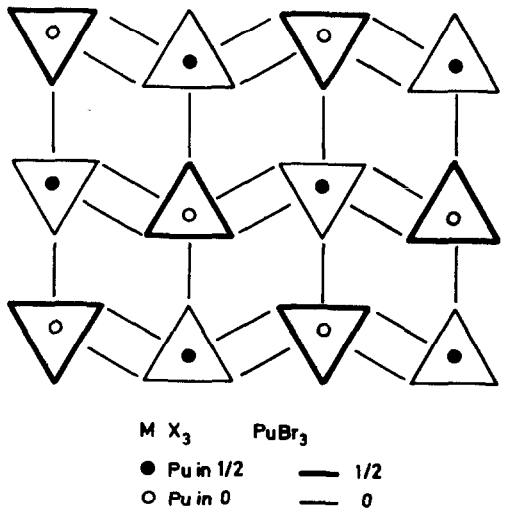

FIG. 10. Representation of the $PuBr_3$ structure in a way similar to Fig. 9.

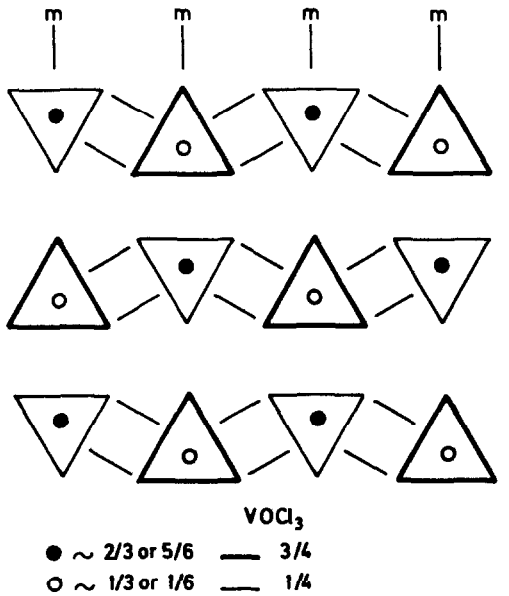

FIG. 11. Representation of the $VOCl_3$ structure as in $AsBr_3$ and $PuBr_3$ structure types.

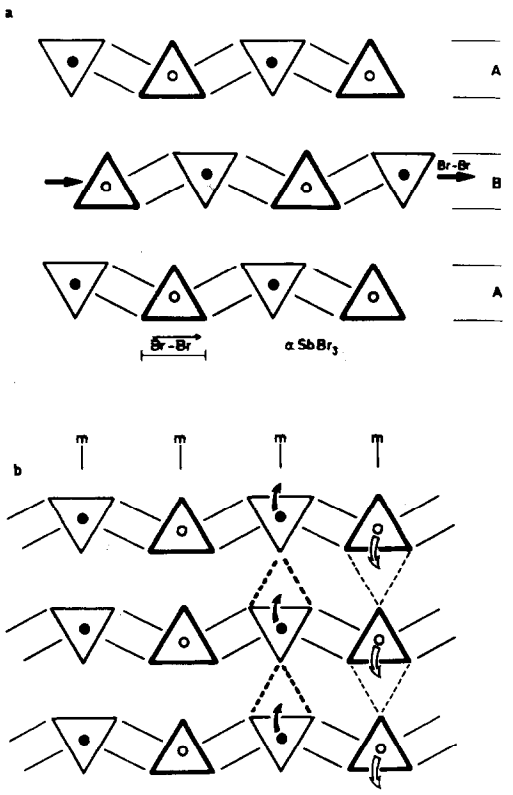

FIG. 12. Mechanism of the transformation $\alpha SbBr_3 \rightarrow \beta SbBr_3$: (a) Displacement of the layer B by a Br–Br vector. (b) Situation after the displacement; infinite chains of empty trigonal prisms created (dashed lines) in the right portion; the arrows indicate the diffusion route of SbE.

$\alpha BiBr_3$ crystallize in the cubic system (Table I). Their crystal structure may possibly be derived from αBiF_3, but a more thorough study is needed to prove such a hypothesis.

III. M^*I_3 Triiodides

All Group VA triiodides, solid at room temperature, are characterized by an hexagonally close packed array (HCP) of the iodine atoms. An exception is provided by one form of the arsenic triiodide, βAsI_3, which exhibits a cubic close packing (CCP).

The HCP family, i.e., PI_3, αAsI_3, SbI_3, and BiI_3, contains two different structural

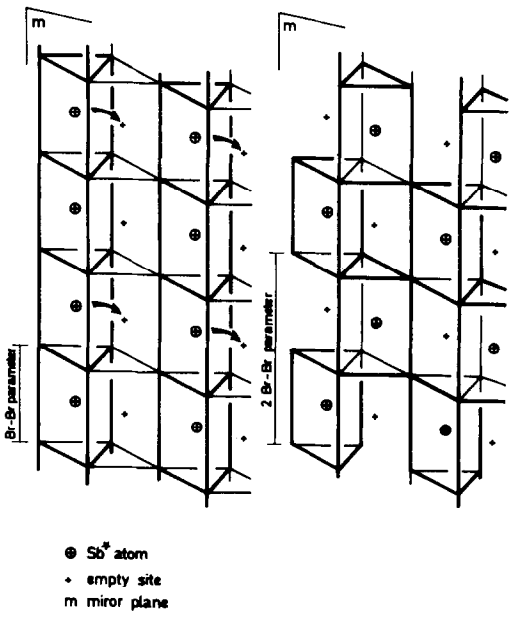

FIG. 13. A detailed picture of the infinite chains in $\alpha SbBr_3$ (on the left) and in $\beta SbBr_3$ (on the right).

classes: the PI_3 structure type and the αAsI_3 structure type.

In both these types, the element M^*, with its lone pair E, is situated in an iodine octahedron.

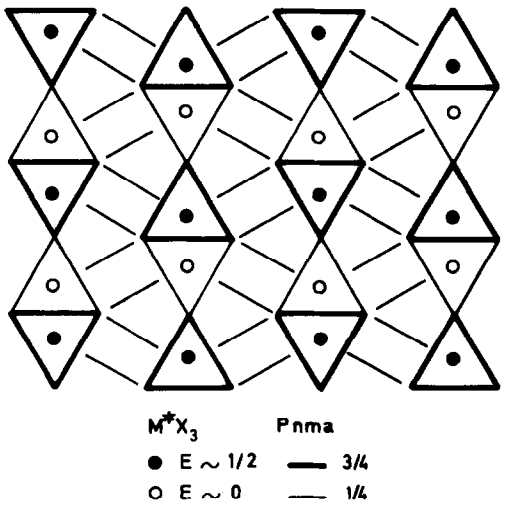

FIG. 14. Idealization of the YF_3 structure type of $\beta SbBr_3$ and resulting structure after the transformation described in Figs. 12a and b; (projection parameter 2(Br–Br) distance).

These structures are better understood using the schematic representation developed by Andersson and Galy (*42*) describing Wadsley's defects and crystallographic shears in hexagonally close packed structures. Figure 15 shows the different ways of joining the octahedra in a HCP arrangement.

PI_3—A Structural Type

The crystal structure of phosphorus triiodide was originally investigated by Braekken (*43*) who determined the iodine atom positions. However, the phosphorus positions were not resolved. Wyckoff (*14*) indicated that the phosphorus atom, similarly to the boron of the isostructural compounds BCl_3, BBr_3, and BI_3, is located in the middle of the halide triangle. Such an assertion is unreasonable in the case of phosphorus(III), since the size of the site is too small to accommodate the P atom with its lone pair. This assignment is also unrealistic for the molecular structure.

The crystal structure of PI_3 was reinvestigated by Lance *et al.* (*44*). The phosphorus atoms were shown to be situated above the planes of a nearly ideal HCP of iodine atoms, and the pyramidal geometry of the molecule is maintained inside the solid (Fig. 16, Table I). The stereochemical influence of the lone pair is clearly indicated: the structure is isostructural with triiodomethane (*45*). The phosphorus atom and its lone pair are located in the octahedral iodine site. These octahedra appear as some kind of zig-zag chains along the *c* axis connected to each other by sharing adjacent corners (Fig. 17).

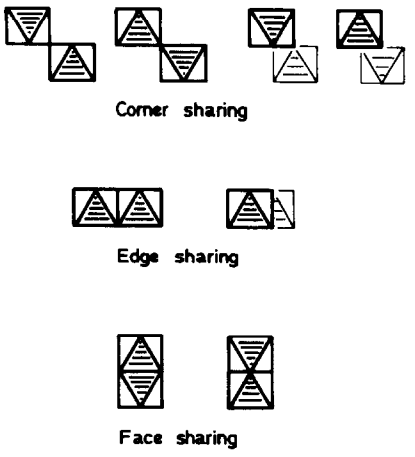

FIG. 15. A few possible ways of joining octahedra when the projection axis is $a + b$ in the hexagonally close packed arrangement of iodine atoms.

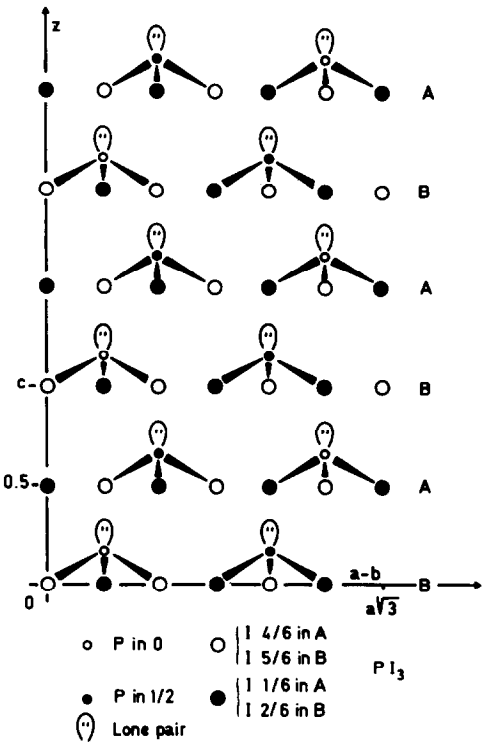

FIG. 16. The projection of the PI_3 structure onto the plane (110).

Among the M^*X_3 structure types, both PI_3 and VF_3 constitute examples where only one-third of the octahedral holes of HCP are occupied. The ideal VF_3 structure type is given in Fig. 18 to facilitate the comparison (*14, 42*).

αAsI_3—A Structural Type

AsI_3—the α form. The refinement (R = 0.033) of the crystal structure of αAsI_3 has been recently reported (*46*). In 1931, Hey-

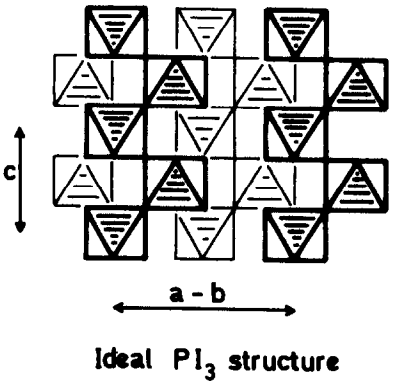

FIG. 17. The PI_3 structure type.

worth (*47*) published the original structure with pertinent comments concerning the arsenic stereochemistry. Later on, Trotter's work (*48*) confirmed both the structure and the remarks in spite of the poor reliability factors obtained ($R = 0.11$ and $R = 0.16$ for $hk0$ and $h0l$ film data).

The structure can be described as constituted of discrete AsI_3 molecules; the As atoms and their lone pair E are located in two out of three octahedra every two layers (A, B) of the hexagonal close packing of iodine atoms (Fig. 19):

$$\ldots\ldots A - (AsE)_2 - B - A - (AsE)_2 - B - A - (AsE)_2 - B - A \ldots\ldots$$

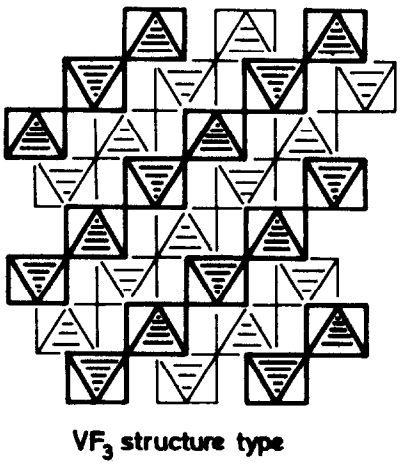

FIG. 18. The VF_3 structure type.

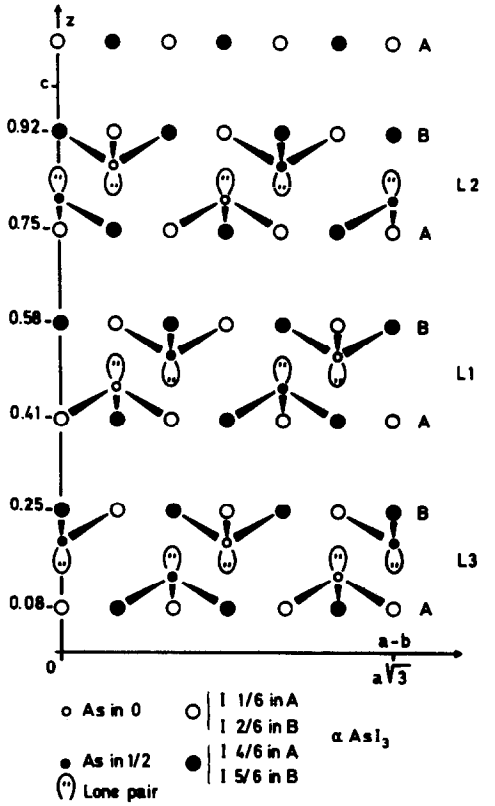

FIG. 19. The projection of αAsI_3 structure onto the plane (110).

The ideal drawing of the αAsI_3 structure (Fig. 20) shows the arrangement of filled iodine octahedra sharing edges and corners.

SbI_3. The crystal structure determination of SbI_3 was performed by Trotter and Zobel (*49*) using X-ray photographic data. SbI_3 is isostructural with AsI_3 (Table I).

BiI_3. BiI_3 is commonly referred to in the literature as a structural type, which obviously overlooks the original work on the α form of AsI_3 by Heyworth (*47*).

Nevertheless, from the powder pattern analysis, Trotter and Zobel (*49*) claimed the bismuth(III) to be in the center of the iodine octahedron which implied that the molecular form BiI_3, as in the preceding iodides, was no longer present in the solid.

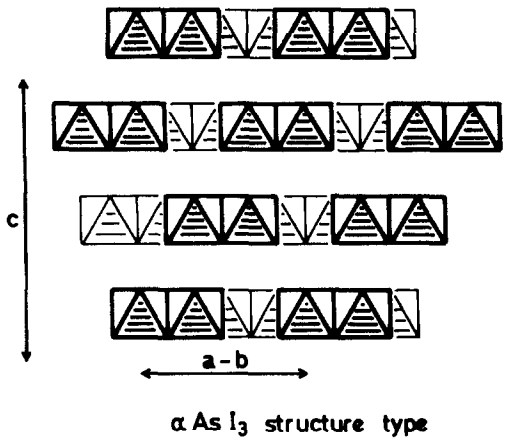

FIG. 20. The αAsI_3 structure type.

Our own interest in the "lone pair element" stereochemistry prompted us to reexamine this question. We started growing single crystals of BiI_3 and studying them by X-ray techniques. Partial results have now been obtained concerning its crystal structure (crystal data in Table I) which may be briefly summarized: (1) the tripling of the c axis is confirmed although some authors report $a = 7.50, c = 6.9$ Å (*14*), (2) the iodine packing is HCP, and (3) the calculations indicate that the bismuth atoms seem to occupy most of the octahedral sites in a nonstoichiometric way, in spite of a preference for the αAsI_3 distribution type of atoms.

Further work is needed, to control the crystal growing and annealing. The possibility of an ordered phase with the c parameter ca. 7 Å and of another phase with a triple c value, as well as of a multiple twinning between the two phases, cannot be excluded.

Polymorphism of AsI_3

The high temperature form AsI_3. αAsI_3, in the form of a deep orange powder, when heated at ca. 110°C in a Pyrex tube yields a pale yellow crystalline phase in the cooler portion of the tube. After a few days at room temperature, this phase turns orange. It obviously transformed back to orange αAsI_3. This "high"-temperature form of AsI_3, already reported by Horiba and Inouye (*50*), is called βAsI_3. AsI_3 therefore exhibits a reversible polymorphic transformation: $\alpha AsI_3 \overset{110°C}{\rightleftarrows} \beta AsI_3$.

X-ray powder analysis. The experiment above was repeated in a Lindemann capillary and a powder pattern of the yellow phase was recorded using the Debye–Scherrer technique (Cu$K\alpha$ radiation). The interplanar distances of the observed diffraction lines, together with the visually estimated intensities, are summarized in Table III.

βAsI_3 structure—a possible $CrCl_3$ type? The βAsI_3 powder pattern is different from that of αAsI_3; nevertheless it can be indexed using an analogous hexagonal cell, with the following parameters: $a = 7.20$ and $c = 21.47$ Å, but the extinction rules are quite different, the major ones being $00l$ $l = 3n + 1$.

From a thorough NQR study on the β phase by Kojima *et al.* (*51*), this crystalline phase is claimed to contain three crystallographically independent iodine atoms. Up to 383 K, only one signal is obtained ($\nu_1^{127}I = 207.023$ MHz), showing the three iodine atoms of the molecule to be crystallographically equivalent in the αAsI_3 structure type. Above this temperature, three distinct signals appear ($\nu_1^{127}I = 206.20$, 208.45, and

TABLE III

AsI_3 POWDER PATTER

$I_{obs.}$	$d_{obs.}$ (Å)	$d_{calc.}$ (Å)	$h\ k\ l$
w	3.57	3.578	0 0 6
w	3.40	3.413	1 1 2
vS	3.225	3.216	1 1 3
w	3.016	2.994	0 2 2
		2.990	1 1 4
S	2.554	2.538	1 1 6
S	2.078	2.078	0 3 0
w	1.970	1.968	1 2 6
mS	1.789	1.789	0 0 12

211.74 MHz), supporting the conclusions made by these authors (*51*).

The answer to the βAsI_3 structural problem could then be assumed by the $CrCl_3$ structure type determined by Natta (*52*) and refined by Wooster (*53*), which requires cell parameters similar to αAsI_3 but with space group $P3_212$ (or its enantiomorphic form $P3_112$) which imposes the extinction $00l$ $l = 3n + 1$.

βAsI_3 could then be described with such a structure. The iodine atoms are cubic closed packed and the AsE groups are located in the octahedral sites. As in αAsI_3, two-thirds of the octahedra are filled within one layer formed by iodine atoms and with vacant contiguous layers.

Of course, the arsenic atoms are shifted toward one face of the octahedron as in αAsI_3 as to form molecular entities (Fig. 21). The ideal representation of such a structure is given in Fig. 22 in terms of $CrCl_3$ structure type.

It should be noted that this βAsI_3 structure exhibits a packing (CCP) less dense than the αAsI_3 form (HCP).

Proposal for the mechanism of the phase transition. The comparison of the two idealized Figs. 20 and 22 generates a simple proposal for the phase transition mechanism. The identity of the layers L1 (Figs. 19 and 21) should be mentioned. To get the β form from the α form, layers L2 and L3 just have to moved, and reversely. This scheme is indicated in Fig. 23 for the $\alpha \rightarrow \beta$ transition:

(1) the layers L1 are kept in their original position

(2) the layers L2 are shifted by a vector with a $2a/6$ modulus in the direction $\{110\}$, i.e., $\overrightarrow{2a/6\ \{110\}}$

(3) the layers L3 are shifted by a vector with a $a/6$ modulus in the direction $\{110\}$ and $a\sqrt{3}/6$ in the direction $\{\bar{1}10\}$, i.e.: $\overrightarrow{a/6\ \{110\}} + \overrightarrow{a\sqrt{3}/6\ \{\bar{1}10\}}$.

After this operation, Fig. 22 is derived from Fig. 20. Such a mechanism requires only weak forces to act, as the layers L1, L2, and L3 are separated by vacant layers in which only van der Waals bonds exist. This driving force is readily obtained by gentle heating ca. 110°C, to transform $\alpha \rightarrow \beta$. After a few days at room temperature, $\beta \rightarrow \alpha$. The kinetics of such a transformation is accelerated greatly by heating the sample ca. 80°C.

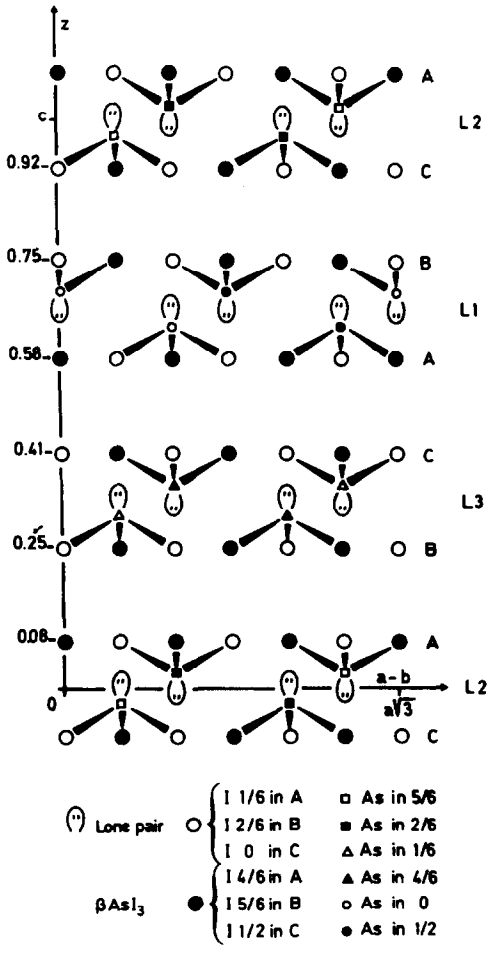

FIG. 21. The projection of the βAsI_3 structure onto the plane (110) proposed after the $CrCl_3$ structure type.

A possible high pressure form for M^*I_3 (αAsI_3 structure type)? In 1969, Andersson and Galy (*54*) proposed a mechanism, by simple cation rearrangement, to explain the way TiO_2(I) (rutile) transforms into TiO_2(II) (αPbO_2 structure type) under high pressure

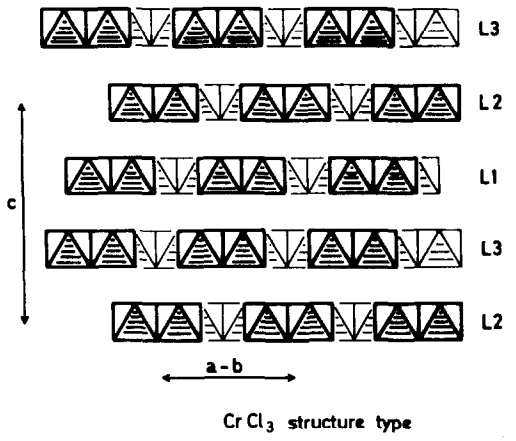

FIG. 22. Ideal representation of the βAsI_3 structure with the $CrCl_3$ structure type.

(Fig. 24). Such a mechanism was later confirmed in an experiment performed by Colaitis and Lecaille (*55*) who studied the transformation of ReO_2 (rutile) → ReO_2 (αPbO_2) using electron microscopy. Similar mechanisms were also successfully proposed to relate Li_2ZrF_6, trirutile, and Na_2SiF_6 structure types, and to follow more easily the phase transitions of the compounds with the general formula AB_2X_6 in a pressure–temperature phase diagram (*56*).

If pressure is applied on a triiodide with the αAsI_3 structure type, the repulsion between M^*–M^* may be increased because of a new repartition requiring the occupation of the empty layers in order to obtain the

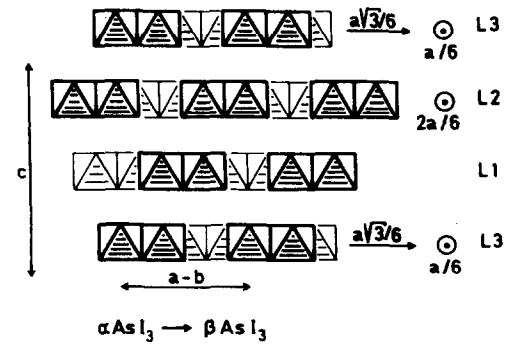

FIG. 23. Proposed mechanism for the $\alpha \rightarrow \beta AsI_3$ transformation (projection onto the plane (110)).

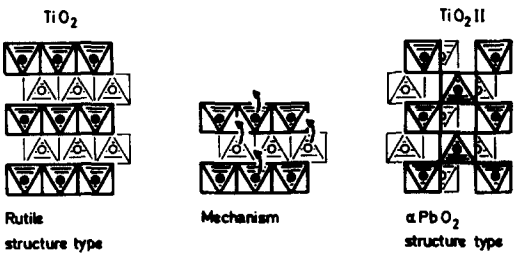

FIG. 24. The mechanism for the rutile → αPbO_2 transformation.

most important interatomic distances between M^* atoms. Such a possibility is illustrated by Fig. 25 where the arrows indicate the diffusion route of half the M^* atoms through the faces of iodine octahedra to occupy the neighboring empty layers. Such a mechanism would involve a cooperative phenomenon.

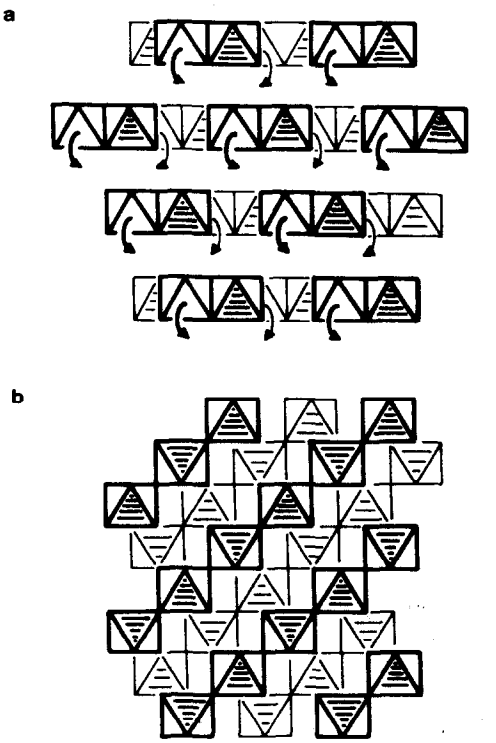

FIG. 25. Proposal for a possible high-pressure transformation of αAsI_3: (a) αAsI_3; the diffusion way of the atoms is indicated by the arrows. (b) Hypothetical AsI_3 high-pressure form isostructural with VF_3.

The resulting structure is actually simple, i.e., the VF_3 type in which the filled octahedra share only corners.

IV. M^*X_3 Molecules and Lone Pair Stereochemistry

As already stated, the trihalides of the VA elements, M^*X_3, show molecules entities in the solid state. Their classification in structural types has been achieved, it is interesting to compare the typical bond lengths M^*–X and bond angles X–M^*–X of the molecules in their different states (gas, liquid, or solid).

Where available, the remarkable similarity of the data obtained by various techniques for a given M^*X_3 molecules should be noted (Table IV).

In all these trihalides, M^* and its lone pair E are found in three main different coordination polyhedra (αBiF_3 is the only exception with BiE in a monocapped trigonal antiprism) (Fig. 26):

(1) C.N. 9, as a tricapped trigonal prism examplified by the $AsCl_3E$ case;

(2) C.N. 8, as a bicapped trigonal prism, for which a view of the PBr_3E entity is given;

(3) C.N. 6, as a trigonal antiprism, with the example of the octahedron of iodine in AsI_3E.

All the M^*–X distances included in these coordination polyhedra are summarized in Table V. Such a description, which accounts for all the anions surrounding M^*E, has been presented by Fourcade (*57*) during an original chemical investigation of antimony compounds.

As expected from VSEPR theory (*5*), the bond angles decrease when the electronegativity of M^* decreases (N → Bi) or when that of the ligands X increases (I → F).

Structural Evolution with the Nature of the Ligand X

The interaction between the lone pair borne by M^* and the nature of the anions

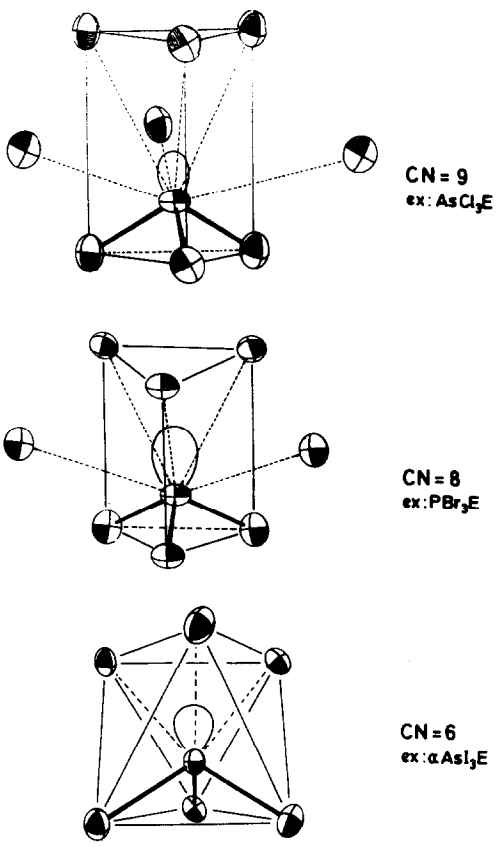

FIG. 26. Coordination polyhedra C.N. 9, 8, and 6.

which comprise the coordination polyhedra are illustrated by the arsenic trihalides (C.N. 9). Figure 27 clearly shows this structural evolution. When X represents the iodine atoms, the important size of the latter makes the "tricapped trigonal prism" as two octahedra sharing one face. When the size of X is smaller, i.e., with bromine and chlorine, the preceding polyhedron is transformed into a tricapped trigonal prism (compression along the pseudo threefold axis to make a regular trigonal prism with $X_{A's}$ and $X_{B's}$ anions, and with $X_{C's}$ slightly displaced from the axis. Such a polyhedron surrounds the arsenic atom and its lone pair E. When fluorine is substituted, the trigonal prism is too small to allow AsE to align itself along its own threefold axis. The arse-

TABLE IV

COMPARISON OF THE M^*X_3 MOLECULAR DATA[a]

	X															
	F				Cl				Br				I			
M^*(VA)		$M-X$	$<X-M-X$	$X-X$		$M-X$	$<X-M-X$	$X-X$		$M-X$	$<X-M-X$	$X-X$		$M-X$	$<X-M-X$	$X-X$
N			NF_3				NCl_3				NBr_3				NI_3	
	ed	1.371	102.2	2.134	*RX*	1.75	106.8	2.82								
P			PF_3				PCl_3				PBr_3				PI_3	
					RX	2.034	100.1	3.119	*RX*	2.213	100.5	3.404	*RX*	2.463	102.0	3.829
	ed	1.570	97.8	2.366	mw	2.040	100.3	3.132	ed mw	2.20	101	3.40	ed	2.43	102	3.78
As			AsF_3				$AsCl_3$				$AsBr_3$				AsI_3	
	RX	1.707	93.9	2.487	*RX*	2.167	97.7	3.265	*RX*	2.364	97.7	3.559	*RX*	2.591	99.7	3.959
	mw	1.706	96.2	2.540	mw	2.161	98.7	3.279	ed	2.33	99.7	3.56	ed	2.557	100.2	3.923
Sb			SbF_3				$SbCl_3$				$SbBr_3$				SbI_3	
	RX	1.92	87.8	2.65	*RX*	2.36	95.2	3.49	*RX* α	2.50	95	3.69	*RX*	2.87	96	4.27
					n	2.35	96	3.49	β	2.49	95	3.69				
					mw	2.325	99.5	3.549	ed	2.51	97	3.76	ed	2.719	99.1	4.138
Bi			BiF_3				$BiCl_3$				$BiBr_3$				BiI_3	
					RX	2.50	91	3.57					*RX*	3.09	83	4.10
					ed	2.48	100	3.80	ed	2.66	100	4.08				

[a] Bond lengths and interatomic distances (Å), bond angles (°). Methods: X-ray (RX), electron diffraction (ed), microwaves (mw), and neutrons (n).

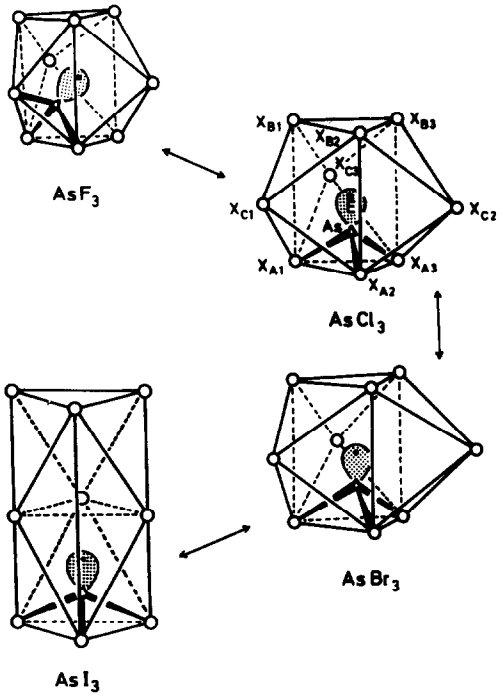

FIG. 27. Correlative evolution of both polyhedra and bonding distribution in the arsenic trihalides crystal structures.

nic atom is then pushed toward one of the capped square pyramids in order to leave as much space as possible in the polyhedron for the nonbonded electron pair and its sphere of influence.

*Structural Behavior of the Elements M**

The M^* cations behave like very big cations (i.e., plutonium in $PuBr_3$) as are entities such as "PO" or "VO" (see POX_3 (X = Cl, Br) and $VOCl_3$ structures), when involved in crystal structures.

This influence of the nature of M^* together with its lone pair is demonstrated by the triiodide structures. Indeed, the separation between iodine planes sandwiching M^*E entities (PI_3, 3.707 Å, AsI_3, 3.669 Å, SbI_3, 3.602 Å, BiI_3, 3.548 Å), clearly indicates that the sphere of influence more closely surrounds M^* when the size of the cation increases. The nature of M^* is also important in the structural evolution of the trichlorides and tribromides. When Z increases, a deviation appears at the level of the arsenic compounds which crystallize with the $AsBr_3$ structure type, whereas NCl_3, PX_3 and BiX_3 crystallize with the YF_3 structure type, and SbX_3 is able to crystallize in both structure types. In the case of arsenic, the new molecular packing, with an unidimensional type, might be due to the d orbital filling, the direction M^*–E being more rigidly determined. Such a pattern is more vague for antimony which allows it to organize its molecular packing in both YF_3 and $AsBr_3$ ways. In the case of bismuth, the partial s character of the lone pair makes BiX_3 crystallize again with the YF_3 structure type. It is to be noted that the volume of $BiCl_3$ is 10% smaller than that of the corresponding $SbCl_3$. Such an outstanding fact indicates that relativistic effects also are acting.

Evaluation of the Stereochemical Influence of the Lone Pair E

It is then tempting to apply the ideas and suggestions developed by Galy *et al.* (*8*) to determine the coordinates of the center E_s of the sphere of influence of the lone pair. E_s is situated at the apex of a trigonal pyramid based on the three halogens and including M^* and the centroïd of the lone pair, designated by E_c, as shown in the scheme given in Fig. 28. Using such methods, the distances M^*–E_s were obtained. The resulting values were compared with the values obtained from a formula proposed in a previous paper by Galy and Enjalbert (*20*):

$$M^*\text{–}E_s = (a_e^2 - a_t^2/3)^{1/2} - (d_t^2 - a_t^2/3)^{1/2}$$

where a_t is the average value of the X–X distances in M^*X_3, $a_e = a_t/2 + 1.30$ Å (1.30 Å is the radius of the sphere of influence of E (*7, 8*)), and d_t is the mean distance M^*–X: N–E_s = 1.50, P–E_s = 1.25, As–E_s = 1.15, Sb–E_s = 1.05, and Bi–E_s = 0.90 Å.

TABLE V

COVALENT AND SECONDARY BOND LENGTHS WITHIN THE COORDINATION POLYHEDRA CONTAINING *M**

	X											
*M**(VA)	F		Cl			Br			I	
	NF_3			NCl_3			NBr_3			NI_3	
				1.79 (×2)	1.78 (×2)						
		1.73 (×2)		1.71 (×1)	1.70 (×1)						
N		1.77 (×1)		3.92 (×2)	3.69 (×2)						
		3.30 (×2)		3.19 (×1)	3.63 (×1)						
		3.36 (×1)		3.96 (×2)	3.89 (×2)						
		CN = 6		*CN* = 8	*CN* = 8						
	PF_3			PCl_3			PBr_3			PI_3	
					2.038 (×2)			2.212 (×2)			
					2.026 (×1)			2.216 (×1)			
P		*CN* = 8			3.852 (×2)	*CN* = 8		3.869 (×2)	*CN* = 6	2.463 (×3)	
					3.612 (×1)			3.754 (×1)		3.670 (×3)	
					3.853 (×2)			3.926 (×2)			
	AsF_3			$AsCl_3$			$AsBr_3$			AsI_3	
		2.940 (×1)			3.773 (×1)			3.738 (×1)			
		3.052 (×1)			3.692 (×1)			3.863 (×1)			
	1.699 (×1)	3.627 (×1)	2.169 (×1)		3.727 (×1)		2.354 (×1)	3.869 (×1)			
As	1.700 (×1)	3.184 (×1)	2.162 (×1)		3.703 (×1)		2.354 (×1)	3.947 (×1)	*CN* = 6	2.591 (×3)	
	1.721 (×1)	3.599 (×1)	2.171 (×1)		3.865 (×1)		2.384 (×1)	4.170 (×1)		3.467 (×3)	
		2.886 (×1)			3.968 (×1)			4.210 (×1)			
	CN = 9		*CN* = 9			*CN* = 9					
	SbF_3			$SbCl_3$			$SbBr_3$			SbI_3	
					α			*β*			
		1.94 (×2)			2.368 (×2)		3.79 (×1)	2.51 (×2)			
		1.90 (×1)			2.340 (×1)	2.46	3.81 (×1)	2.47 (×1)			
Sb	*CN* = 8	2.60 (×2)	*CN* = 8		3.457 (×2)	2.50	3.75 (×1)	3.70 (×2)	*CN* = 8	2.87 (×3)	
		2.63 (×1)			3.609 (×1)	2.54	3.86 (×1)	3.82 (×1)		3.32 (×3)	
		3.93 (×2)			3.736 (×2)		4.09 (×1)	3.88 (×2)			
						CN = 9	4.18 (×1)	*CN* = 8			
	BiF_3			$BiCl_3$			$BiBr_3$			BiI_3	
		2.49 (×3)			2.52 (×2)						
Bi		2.39 (×1)			2.47 (×1)						
	CN = 8	2.59 (×3)	*CN* = 8		3.22 (×2)				*CN* = 6	3.09 (×6)	
		2.69 (×1)			3.26 (×1)						
					3.43 (×2)						

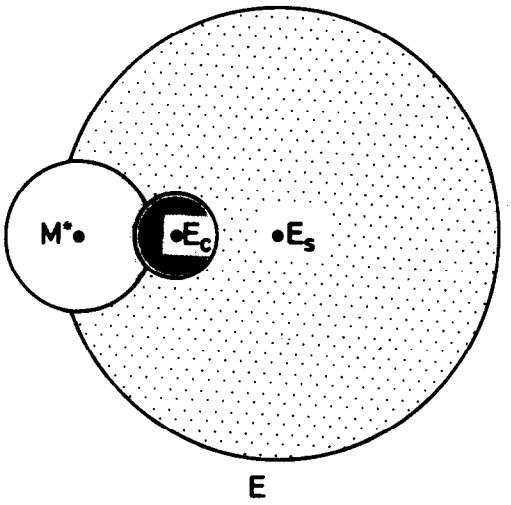

FIG. 28. Schematic representation of the atom M^*, with the centroid E_c and the sphere of influence E_s of the lone pair E.

TABLE VI

M^*–E_s DISTANCE (Å)

		N(III)			
		1.50			
		P(III)	S(IV)	Cl(V)	
		1.25	1.46	1.50	
Ga(I)	Ge(II)	As(III)	Se(IV)	Br(V)	
0.95	1.05	1.26	1.22	1.47	
In(I)	Sn(II)	Sb(III)	Te(IV)	I(V)	Xe(VI)
0.86	0.95	1.06	1.25	1.23	1.49
Tl(I)	Pb(II)	Bi(III)	Po(IV)		
0.69	0.86	0.98	1.06		

A reasonable agreement is found for these calculated M^*–E_s distances with those already published on arsenic, antimony, and bismuth (*8*). Such values derived by applying geometrical principles and by averaging some distances in real crystal structures are probably correct within 0.1 Å.

Another way to obtain these M^*–E_s distances was by calculating the coordinates of the bary-center of the coordination polyhedron around M^* where E_s is supposed to be located.

Good agreement was found with the above values, the results being generally smaller by less than 0.1 Å, but this calculation does not work for the iodides, since their large size and high polarizability make them deviate.

The observed M^*–E_s values are listed in Table VI together with those corresponding to the M^* elements.

From these remarks, it is concluded that: (1) secondary interactions between M^* and X anions of other molecules exhibit shorter distances when Z increases from N to Bi atoms in one column of the periodic table; correlatively, the M^*–E_s values decrease; (2) in other respects, when extending the fundamental results obtained by Schmiedekamp *et al.* (*6*) it appears that the centroïd E_c of the lone pair moves away from the nucleus when passing from nitrogen to bismuth (example: N–E_c = 0.38 Å for NF_3, P–E_c = 0.57 Å for PF_3 (*6*)).

A possible explanation might lie in the ability of the lone pair, when its centroïd is close enough to the nucleus, to screen it and then to make difficult the acting of the secondary interactions in this direction opposite the covalent bond.

When going from top to bottom of the VA column, the nucleus of M^* increases its size and the centroïd of the lone pair is somewhat moved away from its center. The secondary interactions M^*–X can then be established attracting the neighbor molecules to M^* and, by the way, virtually bringing closer to M^* the sphere of influence, which consequently makes M^*–E_s decrease.

With the same basic hypothesis, this explanation can be extended to one row of the periodic table. For example, increasing values of M^*–E_s have also been found in the row In(I) to Xe(VI) (Table VI; Ref. (*8*)). The charge of the nucleus drastically in-

creases from indium to xenon and the nucleus should then attract more and more the electron pair, with correlatively expanding M^*–E_s distances.

Thus the "diagonal rule" of the periodic table is followed and it is readily seen that the Xe–E_s distance is very close to that of N–E_s. Looking at the XeO_3 structure, in which the trigonal prism packing is very distorted compared to the "isostructural" one of AsF_3 (see Fig. 2), it is tempting to consider that if we had a crystal of PF_3 (possible) its crystal structure should be a bit more distorted than that of AsF_3 and that of NF_3 very close to XeO_3 (. . . but . . . NF_3 is solid at a temperature below 66 K).

Appendix I

Crystal Structure of AsF_3

AsF_3 is a liquid at room temperature. It is very sensitive to moisture and very reactive. A droplet was inserted and sealed in a Teflon capillary. The crystal was grown *in situ* on the CAD4 automatic diffractometer using the techniques detailed in Enjalbert's thesis (*10*). The data were collected using Mo $K\alpha$ radiation.

Some crystallographic data are reported in Tables I, IV, and V of the paper and the atom positions and thermal parameters in Table IA.

TABLE IA

AsF_3	(193 K) $Pn2_1a$	a = 7.018(5) x		b = 7.315(6) y	c = 5.205(6) (Å) z	$B^b_{eq.}$ (Å²)
As		0.2862(2)		¼[a]	0.0338(2)	1.7(1)
F1		0.0736(17)		0.3065(19)	−1.005(20)	4.6(2)
F2		0.3077(18)		0.0490(17)	−0.1260(26)	3.7(2)
F3		0.1792(16)		0.1493(16)	0.2956(20)	3.3(2)
	β_{11}(×10⁴)	β_{22}	β_{33}	β_{12}	β_{13}	β_{23}
As	75(3)	103(3)	145(5)	−35(4)	0(2)	28(7)
F1	193(23)	299(41)	330(37)	20(26)	−115(30)	48(3)
F2	241(32)	164(22)	262(41)	−11(21)	61(29)	−79(27)
F3	217(26)	162(20)	189(37)	2(20)	84(24)	8(21)

[a] Polar space group, y is arbitrarily fixed.

[b] $B_{eq-} = \frac{4}{3}\Sigma(\mathbf{a}_i \cdot \mathbf{a}_j)\beta_{ij}$; factor temperature form: $\exp(-(\beta_{11}h^2 + \beta_{22}k^2 + \beta_{33}l^2 + 2\beta_{12}hk + 2\beta_{13}hl + 2\beta_{23}kl))$.

Appendix II

Crystal Structure of $AsCl_3$

A small drop of liquid $AsCl_3$ was placed in a Lindemann capillary and a crystal was obtained using the methods already described (*10*).

Complete data are given in Tables I, IV, and V of this paper and the detailed atomic parameters are listed in Table IIA.

TABLE IIA

$AsCl_3$	(253 K) $P2_12_12_1$	a = 9.466(3) x	b = 11.335(3) y		c = 4.289(2) (Å)	
					z	$B^a_{eq.}$ (Å²)
As		0.3010(1)	0.2879(1)		0.4891(2)	2.62(6)
Cl1		0.2966(2)	0.1236(1)		0.2321(6)	3.2(1)
Cl2		0.1347(2)	0.3792(2)		0.2380(7)	3.4(1)
Cl3		0.4782(2)	0.3676(2)		0.2490(8)	3.4(1)
	$\beta_{11}(\times 10^4)$	β_{22}	β_{33}	β_{12}	β_{13}	β_{23}
As	84(1)	61(1)	231(3)	3(1)	3(3)	−2(2)
Cl1	90(2)	42(1)	578(12)	4(2)	−7(7)	6(4)
Cl2	76(2)	62(2)	564(14)	18(2)	11(6)	3(6)
Cl3	77(2)	62(2)	564(13)	−11(2)	−14(6)	11(6)

[a] $B_{eq.} = \frac{4}{3}\Sigma(\mathbf{a}_i \cdot \mathbf{a}_j)\beta_{ij}$; factor temperature form: $\exp(-(\beta_{11}h^2 + \beta_{22}k^2 + \beta_{33}l^2 + 2\beta_{12}hk + 2\beta_{13}hk + 2\beta_{23}kl))$.

Acknowledgments

The authors wish to thank Pr. Sten Andersson for stimulating and most enjoyable discussions on the subject.

Sincere thanks are also due to Hélène Morelle and Jean-François Kéruzoré for skillful help with the manuscript elaboration and drawing of the figures.

These investigations were supported by the Centre National de la Recherche Scientifique.

References

1. J. GALY, "Solid State Chemistry," Proceedings of the 5th Material Research Symposium, p. 29, NBS special publication 364 (1972).
2. J. ZEMANN, *Monatsch. Chem.* **102,** 1209 (1971).
3. G. MEUNIER, Thèse d'Etat, Université de Bordeaux I, France (1974).
4. N. V. SIDGWICK AND H. M. POWELL, *Proc. R. Soc. London. Ser. A* **176,** 153 (1940).
5. R. J. GILLESPIE AND R. S. NYHOLM, *Q. Rev. Chem. Soc.* **11,** 339 (1957).
6. A. SCHMIEDEKAMP, D. W. J. CRUICKSHANK, S. SKAARUP, P. PULAY, I. HARGITTAI, AND J. E. BOGGS, *J. Amer. Chem. Soc.* **101,** 2002 (1970).
7. S. ANDERSSON AND A. ÅSTRÖM, "Solid State Chemistry," Proceedings of the 5th Material Research Symposium, p. 3, NMS special publication 364 (1972).
8. J. GALY, G. MEUNIER, S. ANDERSSON, AND A. ÅSTRÖM, *J. Solid State Chem.* **13,** 142 (1975).
9. R. ENJALBERT AND J. GALY, *C.R. Acad. Sci.* **C289,** 441 (1979).
10. R. ENJALBERT, Thèse d'Université, Toulouse, France (1980).
11. D. H. TEMPLETON, A. ZALKIN, J. D. FORRESTER, AND S. M. WILLIAMSON, *J. Amer. Chem. Soc.* **85,** 817 (1963).
12. S. ANDERSSON, *Acta Crystallogr.* **B35,** 1321 (1979).
13. J. A. EDWARDS, *J. Chem. Soc. A* 2751 (1970).
14. R. W. G. WICKOFF, "Crystal Structure," Vol. II, 2nd ed., Interscience, New York (1964).
15. F. HUND AND R. FRICKE, *Z. Anorg. Chem.* **258,** 198 (1949).
16. E. I. ARDASHNIKOVA, M. P. BORZENKOVA, F. V. KALINCHENKO, AND A. V. NOVOSELOVA, *Zh. Neorg. Khim.* **26**(7), 1727 (1981).
17. A. ZALKIN AND D. H. TEMPLETON, *J. Amer. Chem. Soc.* **75,** 2453 (1953).
18. S. ANDERSSON AND B. G. HYDE, *J. Solid State Chem.* **9,** 92 (1974).
19. R. ENJALBERT AND J. GALY, *C.R. Acad. Sci.* **C287,** 259 (1978).
20. R. ENJALBERT AND J. GALY, *Acta Crystallogr.* **B35,** 546 (1979).
21. R. ENJALBERT, J. M. SAVARIAULT, AND J. P. LEGROS, *C.R. Acad. Sci.* **C290,** 239 (1980).
22. H. HARTL, S. RAMA, A. SIMON, AND H. J. DIESEROTH, *Z. Nat.* **34b,** 1035 (1979).
23. G. SEMIN, T. A. BABUSHKINA, AND G. G. JACOBSON, "Primenenic Yadernogo Kvadrupol'nogo

Resonansa vo Khimii," Izdatelistvo Khimiya, Leningrad (1972).
24. H. ROBINSON, H. D. DEHMELT, AND W. GORDY, *J. Chem. Phys.* **22,** 511 (1954).
25. K. OLIE, *Acta Crystallogr.* **B27,** 1459 (1971).
26. K. OLIE AND F. C. MIJLHOFF, *Acta Crystallogr.* **B25,** 974 (1969).
27. L. K. TEMPLETON AND D. H. TEMPLETON, *Acta Crystallogr.* **B27,** 1678 (1971).
28. T. OKUDA, K. OSOKAWA, K. YAMADA, Y. FURUKAWA, AND H. NEGITA, *Inorg. Chem.* **14,** 1207 (1975).
29. I. LINDQVIST AND A. NIGGLI, *J. Inorg. Nucl. Chem.* 345 (1956).
30. D. W. CUSHEN AND R. HULME, *J. Chem. Soc.* **427,** 2218 (1962).
31. A. LIPKA, *Acta Crystallogr.* **B35,** 3020 (1979).
32. S. C. NYBURG, G. A. OZIN, AND J. T. SZYMANSKI, *Acta Crystallogr.* **B27,** 2298 (1971).
33. H. HARTL, J. SCHÖNER, J. JANDER, AND H. SCHULZ, *Z. Anorg. All. Chem.* **413,** 61 (1975).
34. H. BRAEKKEN, *Kgl. Norske Videnskab Selskab* **8,** nr. 10 (1935).
35. A. K. SINGH AND S. SWAMINATHAN, *Curr. Sci.* **33,** 429 (1934).
36. J. TROTTER, *Z. Krist.* **122,** 230 (1965).
37. A. K. SINGH AND S. SWAMINATHAN, *Z. Krist.* **124,** 375 (1967).
38. D. W. CUSHEN AND R. HULME, *J. Chem. Soc.* **798,** 4162 (1964).
39. W. H. ZACHARIASEN, *Acta Crystallogr.* **1,** 265 (1948).
40. R. ENJALBERT, J. STRÄHLE, AND J. GALY, to be published.
41. G. M. WOLTEN AND S. M. MAYER, *Acta Crystallogr.* **11,** 739 (1958).
42. S. ANDERSSON AND J. GALY, *J. Solid State Chem.* **1,** 576 (1970).
43. H. BRAEKKEN, *Forh. K. Nor. Vidensk. Selsk* **5,** 202 (1933).
44. E. T. LANCE, J. M. HASCHKE, AND D. R. PEACOR, *Inorg. Chem.* **15,** 780 (1976).
45. T. L. KITAIGORODSKII AND Y. T. STRUCHKOV, *Zh. Fiz. Khim.* **27,** 647 (1953).
46. R. ENJALBERT AND J. GALY, *Acta Crystallogr.* **B36,** 914 (1980).
47. D. HEYWORTH, *Phys. Rev.* **38,** 351 (1931).
48. J. TROTTER, *Z. Krist.* **121,** 81 (1965).
49. J. TROTTER AND T. ZOBEL, *Z. Krist.* **123,** 67 (1966).
50. S. HORIBA AND R. INOUYE, d'aprés "Nouveau Traité de Chimie Minérale," Paul Pascal, Tome XI. Masson (1958).
51. S. KOJIMA, K. TSUKADA, S. OGAWA, A. SHIMAUCHI, AND Y. ABE, *J. Phys. Soc. Japan* **9,** 805 (1954).
52. G. NATTA, *Rend. Accad. Lincei* **5,** 592 (1927).
53. N. WOOSTER, *Z. Anorg. Allg. Chem.* **189,** 329 (1930).
54. S. ANDERSSON AND J. GALY, *Bull. Soc. Chim. Fr.* **194,** 1065 (1969).
55. D. COLAITIS AND C. LECAILLE, *Mat. Res. Bull.* **7,** 369 (1972).
56. J. GALY AND S. ANDERSSON, *J. Solid State Chem.* **3,** 525 (1971).
57. R. FOURCADE, Thèse d'Etat, Univ. de Montpellier, France (1975).